

# 1 Alkalinity sources in the Dutch Wadden Sea

## 2 ~~Distribution and source attribution of alkalinity in the Dutch Wadden Sea~~

3 Mona Norbistrath<sup>1,2,3</sup>, Justus E. E. van Beusekom<sup>1</sup>, & Helmuth Thomas<sup>1,2</sup>

4 <sup>1</sup>Institute of Carbon Cycles, Helmholtz-Zentrum Hereon, Geesthacht, 21502, Germany

5 <sup>2</sup>Institute for Chemistry and Biology of the Marine Environment (ICBM), Carl von Ossietzky University Oldenburg,  
6 Oldenburg, 26129, Germany

7 <sup>3</sup>now at: Department of Marine Chemistry and Geochemistry, Woods Hole Oceanographic Institution, Woods Hole, MA,  
8 02543, USA

9 *Correspondence to:* Mona Norbistrath (mona.norbistrath@whoi.edu)

Formatiert: Hochgestellt

### 10 **Abstract**

11 ~~As the major global CO<sub>2</sub> sink,~~ The oceanic buffering capacity total alkalinity (TA), ~~as the major global CO<sub>2</sub> sink,~~ is of growing  
12 scientific interest. TA is mainly generated by weathering, and further by various anaerobic metabolic processes. The Wadden  
13 Sea, located in the southern North Sea is ~~hypothesized thought~~ to be a source of TA for the ~~carbonate system of the~~ North Sea,  
14 but quantifications are scarce. ~~Here, we observed~~ This study observed TA, dissolved inorganic carbon (DIC), and nutrients in  
15 the Dutch Wadden Sea in May 2019. ~~Along several transects, surface samples were taken to investigate spatial distribution~~  
16 ~~patterns and to compare them with data from the late 1980s. We sampled transect surface waters to detect spatial distributions~~  
17 ~~and compared it with earlier data.~~ A tidal cycle was sampled to further shed light on TA generation and potential TA sources.  
18 We identified the Wadden Sea as a source of TA with an average TA generation of 7.6  $\mu\text{mol kg}^{-1} \text{h}^{-1}$  TA during ebb tide in the  
19 Ameland Inlet. TA was generated in the sediments ~~with deep pore-water flow during low tide enriching the surface water, and~~  
20 ~~washed out with off-running water.~~ A combination of anaerobic processes and CaCO<sub>3</sub> dissolution were potential sources of  
21 TA in the sediments. We assume that seasonality and the associated nitrate availability in particular influence TA generation  
22 by denitrification, which we assume is low in spring and summer.

### 23 **1 Introduction**

24 ~~As the regulator of the ocean carbon dioxide (CO<sub>2</sub>) sink,~~ Total alkalinity (TA) is of increasing scientific interest ~~as the regulator~~  
25 ~~of the ocean carbon dioxide (CO<sub>2</sub>) sink,~~ and is investigated worldwide in the Anthropocene (Abril and Frankignoulle,  
26 2001;Bozec et al., 2005;Chen and Wang, 1999;Dickson, 1981;Middelburg et al., 2020;Norbistrath et al., 2022;Renforth and  
27 Henderson, 2017;Thomas et al., 2004;2009;Sabine et al., 2004). The Anthropocene describes the current era of our planet,  
28 when environmental changes, driven by humans, have become identifiable in geological records (Zalasiewicz et al.,  
29 2010;Crutzen, 2002). ~~The climate and the increasing atmospheric CO<sub>2</sub> content is mainly regulated by the open ocean. Around~~

Formatiert: Tiefgestellt

30 ~~30 % of the global anthropogenic CO<sub>2</sub> emissions are removed by the ocean~~ (Gruber et al., 2019). ~~The carbon storage capacity~~  
31 ~~of the North Sea is an important atmospheric CO<sub>2</sub> sink as it exports the absorbed CO<sub>2</sub> in the deep layers of the Atlantic Ocean~~  
32 ~~where it is stored on longer time scales~~ (Borges et al., 2005;Bozec et al., 2005;Burt et al., 2016;Brenner et al., 2016;Hu and  
33 Cai, 2011;Schwichtenberg et al., 2020;Thomas et al., 2004;2009). ~~Two important aspects of the oceanic climate regulation are~~  
34 ~~the oceanic circulation and TA. Both interact well in highly active ocean areas such as coastal zones, and shallow areas like~~  
35 ~~continental and marginal shelves. In these shallow areas, TA is very susceptible due to various metabolic processes and the~~  
36 ~~influence of adjacent zones like rivers, estuaries, marshes, and tidal flats~~ (e.g., Norbistrath et al., 2022;2023;Wang et al.,  
37 2016;Voynova et al., 2019). ~~A previous study by Norbistrath et al. (2022) showed that an enhanced riverine, metabolic alkalinity~~  
38 ~~would lead to increasing CO<sub>2</sub> absorption in the coastal zones of the North Sea, highlighting the need to further investigate TA~~  
39 ~~regulation in adjacent zones of coastal oceans.~~

Formatiert: Tiefgestellt

40 Coastal ~~zones~~regions, which are the direct interface between most, if not all, compartments of the Earth system (i.e., terrestrial,  
41 aquatic, oceanic) and human societies, appear particularly vulnerable to environmental and climate change (Glavovic et al.,  
42 2015). This holds true for the Wadden Sea, the shallow, coastal sea along an approximately 500 km coastline of the  
43 Netherlands, Germany, and Denmark, in the southern North Sea, which is declared as an UNESCO world natural heritage site  
44 since 2009. Most ~~of the Wadden Sea part of it~~ is located between the protecting barrier Islands and the Mainland, which makes  
45 it ~~a unique and~~ the world's largest uninterrupted stretch of tidal flats with multiple tidal inlets (Fig. 1). Due to the topography,  
46 the Wadden Sea is a highly dynamic ecosystem with influences from the mainland and the North Sea (Hoppema, 1993;Postma,  
47 1954;van Raaphorst and van der Veer, 1990). Driving forces of the ~~biogeochemical~~ dynamics in the Wadden Sea are nutrient  
48 and organic matter (OM) imports by rivers; ~~and~~ high suspended particulate matter (SPM) imports ~~from~~by the North Sea (Van  
49 Beusekom et al., 2012;Postma, 1954). ~~Physical sources of variability in the Wadden Sea are and~~ oceanic driven wind, waves,  
50 and tidal currents, as well as the counterclockwise circulation of the North Sea (Elias et al., 2012). Large tidal amplitude and  
51 currents in conjunction with shallow water depths allow for vertical water column mixing and an exchange between the benthic  
52 and pelagic realms ~~including deep pore-water exchange~~ (Røy et al., 2008). The high tidal currents also impact the  
53 biogeochemistry of the North Sea (Postma, 1954), as they cause an ~~strong~~ exchange of water ~~masses~~between the North Sea  
54 ~~and the Wadden Sea and play an important role in the import of particulate matter from the North Sea~~ (Burchard et al., 2008).  
55 ~~The North Sea and its carbon storage capacity is an important atmospheric CO<sub>2</sub> sink by exporting and storing the absorbed~~  
56 ~~CO<sub>2</sub> in the deep layers of the Atlantic Ocean~~ (Schwichtenberg et al., 2020;Thomas et al., 2004;2009;Burt et al., 2016;Borges  
57 et al., 2005;Hu and Cai, 2011;Brenner et al., 2016).  
58 ~~TA, primarily consisting of bicarbonate and carbonate, is generated by~~ ~~Next to~~ chemical rock weathering (Suchet and Probst,  
59 1993;Meybeck, 1987;Berner et al., 1983), ~~and TA, usually consisting of bicarbonate and carbonate, is also generated~~ in various  
60 stoichiometries by calcium carbonate (CaCO<sub>3</sub>) dissolution and anaerobic metabolic processes, such as denitrification, which  
61 is the reduction process of nitrate to dinitrogen gas in the nitrogen cycle (Hu and Cai, 2011;Wolf-Gladrow et al., 2007;Chen  
62 and Wang, 1999;Brewer and Goldman, 1976). Understanding of TA sources have recently become increasingly important due  
63 to increasing anthropogenic CO<sub>2</sub> emissions, and the resulting demand for ocean based net-negative CO<sub>2</sub> emissions (e.g., Keith

Formatiert: Tiefgestellt

64 et al., 2006;Matthews and Caldeira, 2008;Zhang et al., 2022). In previous studies, the Wadden Sea was ~~identified~~estimated as  
65 a TA source of the North Sea with a loading between 39 Gmol yr<sup>-1</sup> (Schwichtenberg et al., 2020) and 73 Gmol yr<sup>-1</sup> (Thomas  
66 et al., 2009). Both studies suggested the entire Wadden Sea as one of the most important TA sources of the carbon storage  
67 capacity of the North Sea. Burt et al. (2016) highlighted the importance of coastal TA production for regulating the buffer  
68 system in the North Sea, ~~and whereby they suggested~~ denitrification as the major TA source. Due to the strong connection  
69 between the North Sea and the Wadden Sea, a better understanding of TA generation in the latter ~~one~~ is required. Here, we  
70 focus on the Dutch Wadden Sea that has been well-studied during the past decades (Hoppema, 1990, 1991, 1993;De Jonge et  
71 al., 1993;Elias et al., 2012;Ridderinkhof et al., 1990;Postma, 1954;Van Beusekom et al., 2019;Schwichtenberg et al., 2017).  
72 In particular Hoppema (1990);(1993) observed the spatial and temporal variability of TA in May, which we compare with our  
73 observed transect data to detect potential differences over the last 30 years. In addition, we further shed light on potential TA  
74 sources in the Dutch Wadden Sea.

## 75 2 Methods

### 76 2.1 Study site and sampling

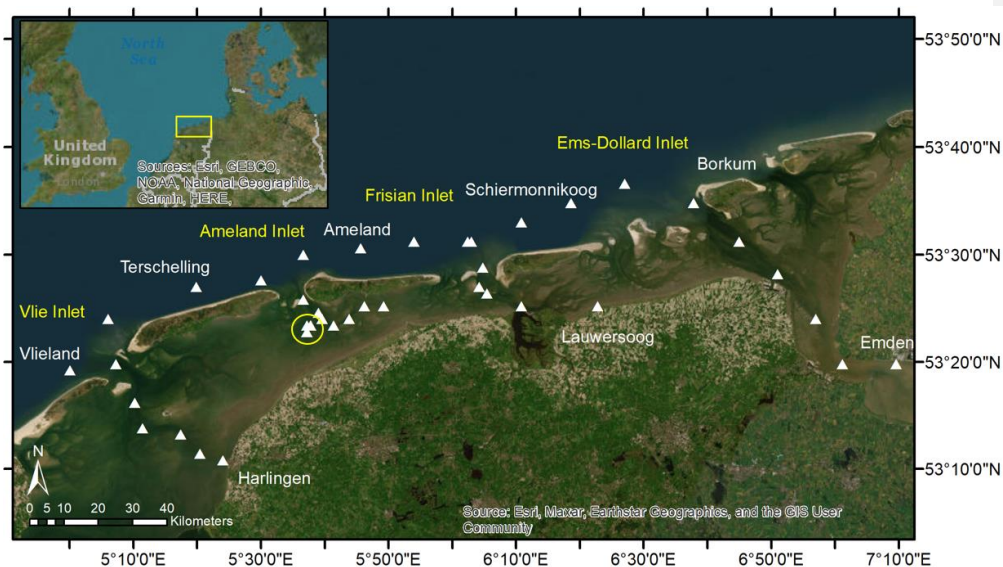
77 This study is based on samples collected on a research cruise (LP20190515) in the Dutch Wadden Sea (Frisian Islands) on RV  
78 *Ludwig Prandtl* in May 2019 (Fig. 1). We collected water samples in the Wadden Sea starting at Harlingen, through the Vlie  
79 Inlet around the islands Vlieland and Terschelling, through the Ameland Inlet to Ameland Island, from there on via the Frisian  
80 Inlet to Lauwersoog, and around Schiermonnikoog Island via the Ems-Dollard Inlet to Emden. In addition, we sampled a tidal  
81 cycle from high tide to low tide (21.05.2019) and from low tide to high tide (23.05.2019) on each day as an anchor station in  
82 the waterway at the western side of Ameland in the Ameland Inlet.

83 Nearly half-hourly, we continuously collected discrete surface (1.2 m depth) water samples with a bypass from the onboard  
84 flow-through FerryBox system (Petersen et al., 2011), which also provided essential physical parameters such as salinity and  
85 temperature. In addition, we sampled a tidal cycle from high tide to low tide and from low tide to high tide on each of two  
86 days as an anchor station in the waterway at the western side of Ameland in the Ameland Inlet.

87 For TA and DIC measurements we sampled water with overflow into 300 mL BOD (biological oxygen demand) bottles and  
88 preserved them with 300 µL saturated mercury chloride (HgCl<sub>2</sub>) to stop biological activity. Each BOD bottle was filled without  
89 air bubbles and closed by using a ground-glass stopper coated in Apiezon® type M grease and a plastic cap. The samples were  
90 stored in a cool dark environment until measurements in the lab.

91 Water for nutrient samples was filtered through pre-combusted (4 h, 450 °C) GF/F filters and the filtrate was stored frozen in  
92 three 15 mL Falcon tubes for triplicate measurements in the lab.

93 In order to determine the total carbon (C), organic carbon (C<sub>org</sub>) and nitrogen (N) concentrations in SPM and associated  
94 C<sub>org</sub>:N ratios, we used pre-combusted (4 h, 450 °C) GF/F filters, which ~~were~~ dried after sampling at 50 °C to remove all  
95 humidity and were stored frozen afterwards until measurement.



97

98 **Figure 1** Sampling site in the Dutch Wadden Sea. The sampling stations around the Frisian Islands in May 2019 are visualized  
 99 with the white triangles. The yellow circle highlights the anchor stations for the tidal cycle sampling in the Ameland Inlet  
 100 two days. During the sampling day from low tide to high tide, we had two samples that we took slightly more western due to  
 101 drifting. The island and city names are shown in white, the inlets in yellow. The tidal flats and sedimentary structures are well  
 102 visible between the barrier islands and the mainland.

## 103 2.2 Sampling and Carbon species analysis

### 104 2.2.1 Carbon species

105 For carbon measurements we sampled water with overflow into 300 mL BOD (biological oxygen demand) bottles and  
 106 preserved them with 300  $\mu$ L saturated mercury chloride ( $HgCl_2$ ) to stop biological activity. Each BOD bottle was filled without  
 107 air bubbles and closed by using a ground glass stopper coated in Apiezon® type M grease and a plastic cap. The samples were  
 108 stored in a cool dark environment until measurements in the lab.

109 The parallel analyses of TA and DIC were carried out by using the VINDTA 3C (Versatile Instrument for the Determination  
 110 of Total dissolved inorganic carbon and Alkalinity, MARIANDA - marine analytics and data), which measures TA by  
 111 potentiometric titration and DIC by coulometric titration with a measurement precision  $< 2 \mu mol kg^{-1}$ . (Shadwick et al., 2011).

112 To ensure a consistent calibration of both measurements, ~~we used~~ certified reference material (CRM batch # 187) provided by  
113 Andrew G. Dickson (Scripps Institution of Oceanography) ~~was used~~.  
114 The calcite ~~and aragonite~~ saturation states ( $\Omega$ ) and the pH were computed with the CO<sub>2</sub>SYS program (Lewis and Wallace,  
115 1998), using the measured parameters TA, DIC, salinity, temperature, silicate and phosphate as input variables, together with  
116 the dissociation constants from Mehrbach et al. (1973), as refit by Dickson and Millero (1987).

### 117 ~~2.3.2~~ Nutrient analyses

118 ~~Water for nutrient samples was filtered through pre-combusted (4 h, 450 °C) GF/F filters to store them afterwards frozen in~~  
119 ~~three 15 mL Falcon tubes for triplicate measurements in the lab.~~

120 ~~We measured~~ The nutrients ~~were measured~~ with a continuous flow automated nutrient analyzer (AA3, SEAL Analytical) and  
121 a standard colorimetric technique (Hansen and Koroleff, 2007) for nitrate (NO<sub>3</sub><sup>-</sup>), nitrite (NO<sub>2</sub><sup>-</sup>), phosphate (PO<sub>4</sub><sup>3-</sup>), and silicate  
122 (Si), and a fluorometric method (K  rouel and Aminot, 1997) for ammonium (NH<sub>4</sub><sup>+</sup>) (Grasshoff et al., 2009).

123 ~~In order to determine the total carbon (C), organic carbon (C<sub>org</sub>) and nitrogen (N) concentrations in SPM and associated C<sub>org</sub>:N~~  
124 ~~ratios, we used pre-combusted (4 h, 450 °C) GF/F filters, which we dried after sampling at 50 °C to remove all humidity and~~  
125 ~~stored frozen until measurement.~~ For the C<sub>org</sub> determination, filters were acidified with 1N HCl and dried overnight to remove  
126 all inorganic carbon content. Filters were measured with a CHN-elemental analyzer (Eurovector EA 3000, HEKAtech GmbH)  
127 in the Institute of Geology, University Hamburg, and calibrated against a certified acetanilide standard (IVA Analystechnik,  
128 Germany). The standard deviations were 0.05 % for carbon and 0.005 % for nitrogen.

### 129 2.4 Data analyses

130 ~~The data analyses were performed by using RStudio Version 1.3.1073    2009-2020 RStudio, PBC. The linear regression~~  
131 ~~Model II was performed by using the “lmodel2” R package, and the plots were created with the “ggplot2” R package.~~

## 132 3 Results

### 133 3.1 Spatial parameter distribution

134 ~~In order to~~ To investigate the spatial distribution of total alkalinity (TA) in the Dutch Wadden Sea and compare its general status  
135 with ~~earlier studies~~ (e.g., Hoppema, 1990) ~~the past~~, we observed the spatial distribution of TA and related parameters from the  
136 coastal mainland towards the open ~~North Sea ocean~~ as surface water transect.

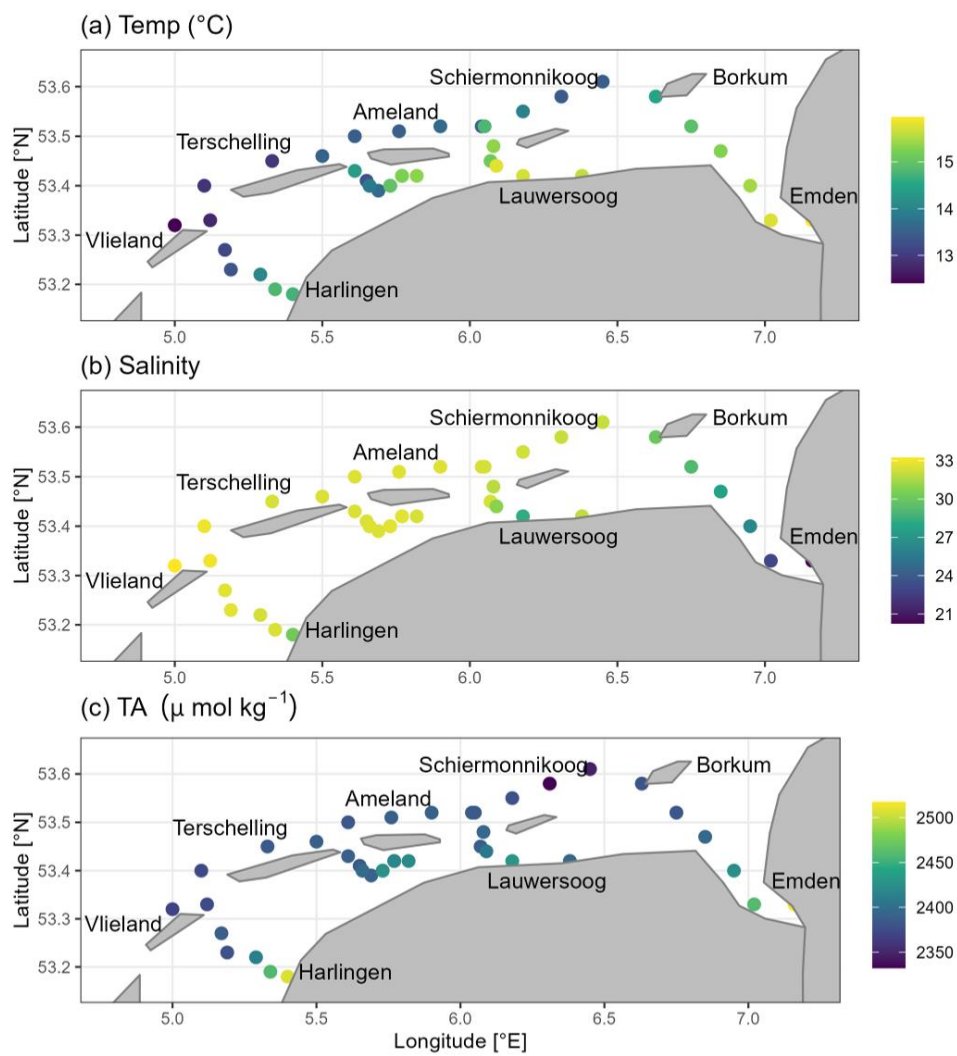
137 The temperatures varied between 12 and 16   C with higher temperatures towards the coastal mainland (Fig. 2a). Salinity was  
138 relatively stable with only minor differences varying from 28 to 33 (Fig. 2b). Lower salinities were only observed in the four  
139 sampling stations in the Ems Estuary with the minimum value of 20.25 at the most upstream station.

140 Spatial transect TA contents ranged from 2332   mol kg<sup>-1</sup> to 2517   mol kg<sup>-1</sup>. We observed lower contents on the oceanic, i.e.,  
141 North Sea side of the Frisian Islands with somewhat higher contents around Ameland (Fig. 2c). In contrast to the oceanic side,

Formatiert:   berschrift 2

Formatiert:   berschrift 2

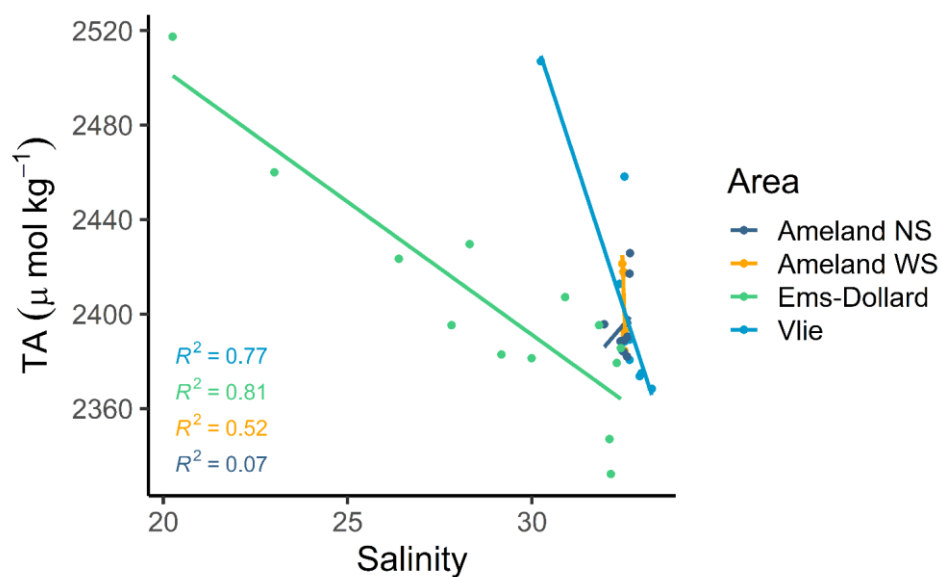
142 the ~~value~~ contents were higher ~~with values~~ ( $> 2380 \mu\text{mol kg}^{-1} \text{TA}$ ) in the Wadden Sea. Only in the Ems Estuary, the contents  
143 were even higher, with values up to  $2517 \mu\text{mol kg}^{-1} \text{TA}$  at the most upstream station. ~~We saw higher~~The TA values ~~were~~  
144 ~~higher~~ in the Wadden Sea than in the open ocean, supporting the assumption of TA being generated in this tidal flat area. ~~We~~  
145 ~~also observed~~ The highest TA contents ~~were observed~~ at the coastal mainland ~~that~~ decreasing towards the North Sea.  
146 ~~In~~ Silicate (Si), ~~we observed~~ showed a similar pattern ~~as in TA~~, with higher concentrations in the Wadden Sea and lower ones  
147 towards the ocean (Fig. A1). Highest concentrations were observed at the coastal mainland and in the Ems Estuary. Silicate  
148 concentrations were between  $0.26$  and  $56.32 \mu\text{mol L}^{-1}$ . ~~Both,~~ The calcite ~~and aragonite~~ saturation states ( $\Omega$ ) ~~was~~ ~~were~~  
149 supersaturated in the entire ~~observed~~ study site ~~(Fig. A2)~~. ~~We observed~~ ~~V~~ values ranged from  $2.32$  to  $4.65$  ~~for calcite (Fig. A2)~~,  
150 ~~and from 1.4 to 3.0 for aragonite (not shown)~~. Highest values were observed at the oceanic side of the barrier islands in the  
151 North Sea. ~~The~~ ~~L~~ lowest values were observed near Harlingen and in the Ems Estuary. ~~Like~~ ~~Similar~~ to the ~~calcite~~ saturation  
152 states ( $\Omega$ ), ~~we observed~~ higher the pH values ~~were higher~~ in the North Sea, and lower ~~values~~ in the Wadden Sea and near the  
153 coastal mainland (Fig. A3). The pH values ranged from  $7.86$  to  $8.19$ . ~~The~~ ~~L~~ lowest values were observed near Harlingen and  
154 in the Ems Estuary. The nitrate ( $\text{NO}_3^-$ ) concentrations were ~~in a similarly similar in a~~ low range ( $< 3 \mu\text{mol L}^{-1} \text{NO}_3^-$ ) ~~throughout~~  
155 ~~in~~ the transect, ~~with~~ ~~h~~ Higher concentrations ( $< 6 \mu\text{mol L}^{-1} \text{NO}_3^-$ ) ~~were observed~~ ~~at~~ ~~only~~ ~~at~~ a few stations close to land, and  
156 maximum concentrations ( $< 38 \mu\text{mol L}^{-1} \text{NO}_3^-$ ) ~~were observed~~ in the Ems Estuary (Fig. A4). ~~Concentrations of DIC contents~~  
157 ranged from  $2097 \mu\text{mol kg}^{-1}$  to  $2430 \mu\text{mol kg}^{-1}$  (Fig. A5). DIC values ~~showed a similar pattern as were similar to~~ TA values,  
158 with higher concentrations near the coastal mainland and in the Ems Estuary, and decreasing concentrations toward the North  
159 Sea, where ~~we observed lowest~~ DIC ~~contents~~ ~~reached minimum values~~.



161 **Figure 2** ~~Spatial distribution of various parameters.~~ Latitudinal and longitudinal distribution of a) temperature ( $^{\circ}\text{C}$ ), b) salinity,  
162 ~~and c) total alkalinity (TA;  $\mu\text{mol kg}^{-1}$ ), d) silicate (Si;  $\mu\text{mol L}^{-1}$ ), e) calcite saturation state ( $\Omega$ ), f) pH, g) nitrate ( $\text{NO}_3^-$ ;  $\mu\text{mol}$   
163  ~~$\text{L}^{-1}$ ), and h) dissolved inorganic carbon (DIC;  $\mu\text{mol kg}^{-1}$ )~~ from surface water samples in May 2019.~~

164  
165 The strong impact from the inner Ems Estuary is visible in all parameters with higher values in the outer estuary and its adjacent  
166 zones, or with lower values in case of pH and the calcite saturation state. Furthermore, we observed higher values around  
167 Ameland Island than in the western part ~~of~~ the transect starting from Harlingen towards the Vlie Inlet. ~~In particular a~~  
168 the oceanic side ~~off~~ from the Vlie Inlet, the impact of the North Sea is visible through lower temperatures and higher salinities.  
169 The North Sea impact is also visible in the mixing between TA and salinity (Fig. 3). ~~We only observed a~~ relatively linear  
170 mixing behavior was only observed in the transect through the Ems-Dollard Inlet and Vlie Inlet ~~(Fig. 3), where. There, we~~  
171 ~~observed decreasing~~ TA contents decreased with increasing salinities from the mainland towards the ocean (Fig. 3). ~~Therefore,~~  
172 ~~we identify~~ ing the Dutch Wadden Sea as ~~being~~ a source of TA. In contrast to the TA content computed for the salinity end-  
173 member in the Ems-Dollard Inlet, we detected higher TA contents around Ameland, both at the North Sea side (Ameland NS)  
174 and the Wadden Sea side (Ameland WS), as well as in the Vlie Inlet, which further support additional TA sources in the  
175 Wadden Sea (Fig. 3). We detected higher TA concentrations than the TA concentration computed for the salinity end member  
176 in the Ems-Dollard Inlet in the oceanic, i.e., North-Sea-side of Ameland (Ameland-NS), in the Wadden-Sea-side of Ameland  
177 (Ameland-WS), and in the Vlie Inlet, indicating towards additional TA sources. The Ameland NS and Ameland WS data  
178 clearly indicated non-conservative behavior with increasing TA contents at ~~and~~ constant salinities.





179

180 **Figure 3** ~~Total alkalinity—salinity mixing~~. Mixing between total alkalinity (TA) and salinity in the oceanic side of Ameland  
 181 and the Frisian Inlet (Ameland NS), in the Wadden Sea site of Ameland (Ameland WS), around Schiermonnikoog and in the  
 182 Ems-Dollard Inlet, and in the Vlie Inlet.

### 183 3.2 Tidal cycle

184 ~~In order to~~ To estimate TA generation in the Dutch Wadden Sea, to shed light on potential TA sources, and to estimate the  
 185 potential TA amount that is exported to the North Sea, we observed a tidal cycle at an anchor station in the Ameland Inlet on  
 186 two days ~~during with the observation of~~ flood tide and ebb tide, respectively. Here, our focus is on ebb tide data that we used  
 187 to identify patterns in the ~~several biogeochemical parameters various parameters~~ in off running water (Table B1). The salinity  
 188 observations allow us to exclude addition by mixing with freshwater sources, since the salinity was constant between 32.50  
 189 and 32.52 (Table B1). We observed Salinity values were in the range of saline waters like similar to water of the North Sea.  
 190 During ebb tide, TA ranged from high tide with  $2387 \mu\text{mol kg}^{-1}$  TA to low tide with  $2438 \mu\text{mol kg}^{-1}$  TA (Fig. 4a). We identified  
 191 an increase of  $51.6 \mu\text{mol kg}^{-1}$  TA ( $\Delta\text{TA}$ ) over a duration of 6.8 h during ebb tide, resulting in a TA increase of  $7.6 \mu\text{mol kg}^{-1}$   
 192  $\text{h}^{-1}$  TA at the sampling location.

193 DIC contents were similar to TA with minimum values at high tide (2172  $\mu\text{mol kg}^{-1}$  DIC) and highest values (2273  $\mu\text{mol kg}^{-1}$  DIC) at low tide. During ebb tide, we observed an increase of 101.3  $\mu\text{mol kg}^{-1}$  DIC ( $\Delta\text{DIC}$ ) resulting in a DIC increase of 14.9  $\mu\text{mol kg}^{-1} \text{h}^{-1}$  DIC (Fig. 4b). DIC increased almost twice as much as TA.

196 Nitrate concentrations approached seawater concentrations with a minimum observed nitrate concentration of 1.26  $\mu\text{mol L}^{-1}$   $\text{NO}_3^-$  and a maximum concentration of 2.17  $\mu\text{mol L}^{-1}$   $\text{NO}_3^-$  (Fig. 4c~~e~~). During ebb tide, nitrate slightly increased by 0.92  $\mu\text{mol L}^{-1}$   $\text{NO}_3^-$  ( $\text{ANO}_3^-$ ), resulting in a nitrate increase of 0.13  $\mu\text{mol L}^{-1} \text{h}^{-1}$   $\text{NO}_3^-$ .

199 In silicate, ~~we detected~~ a similar pattern with low values (1.8  $\mu\text{mol L}^{-1}$  Si) at high tide and increasing concentrations during ebb tide to a maximum of 11.2  $\mu\text{mol L}^{-1}$  Si ~~was detected~~. The silicate increase ( $\Delta\text{Si}$ ) of 9.4  $\mu\text{mol L}^{-1}$  Si resulted in a silicate increase of 1.4  $\mu\text{mol L}^{-1} \text{h}^{-1}$  Si during ebb tide (Fig. 4d~~e~~).

202 Ammonium increased from 3.47  $\mu\text{mol L}^{-1}$   $\text{NH}_4^+$  to 6.22  $\mu\text{mol L}^{-1}$   $\text{NH}_4^+$  during ebb tide (Fig. 4e~~h~~). We observed an ammonium increase ( $\Delta\text{NH}_4^+$ ) of 2.74  $\mu\text{mol L}^{-1}$   $\text{NH}_4^+$  resulting in an increase of 0.4  $\mu\text{mol L}^{-1} \text{h}^{-1}$   $\text{NH}_4^+$ .

204 ~~The salinity observations allow us to exclude conservative mixing for dilution, since the salinity was constant between 32.50 and 32.52 (Fig. 4d). We observed values in the range of saline waters similar to water of the North Sea.~~

206 The calcite and aragonite saturation states had ~~a~~ maximum values ( $\Omega = 3.8 / 2.4$ ) at high tide and decreased to their minimum ~~to 3.1 ( $\Omega = 3.1 / 2.0$ )~~ during ebb tide (Fig. 4f~~e~~, Table B1). The maximum at high tide indicated the influence of the North Sea that ~~decreased during the ebb~~ decreased with off running water.

209 ~~Similar to~~ Like omega, the pH had maximum values (8.07) at high tide and decreased to a minimum (7.93) during ebb tide (Fig. 4g~~f~~). ~~We observed decreasing pH with off running water.~~

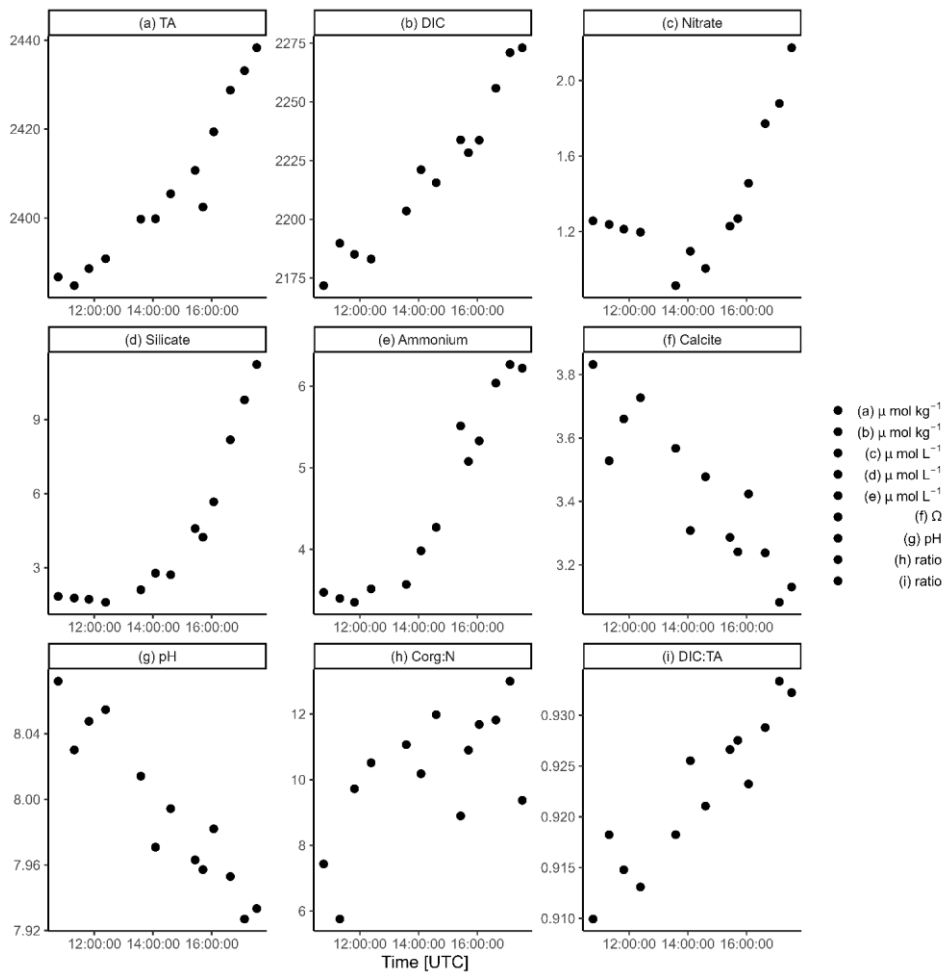
211 ~~Nitrate concentrations approached seawater with a minimum observed nitrate concentration of 1.26  $\mu\text{mol NO}_3^- \text{L}^{-1}$  and a maximum concentration of 2.17  $\mu\text{mol NO}_3^- \text{L}^{-1}$  (Fig. 4g). During ebb tide, nitrate slightly increased by 0.92  $\mu\text{mol NO}_3^- \text{L}^{-1}$  ( $\text{ANO}_3^-$ ), resulting in a nitrate increase of 0.13  $\mu\text{mol NO}_3^- \text{L}^{-1} \text{h}^{-1}$ .~~

214 ~~Ammonium increased from 3.47  $\mu\text{mol NH}_4^+ \text{L}^{-1}$  to 6.22  $\mu\text{mol NH}_4^+ \text{L}^{-1}$  during ebb tide (Fig. 4h). We observed an ammonium increase ( $\Delta\text{NH}_4^+$ ) of 2.74  $\mu\text{mol NH}_4^+ \text{L}^{-1}$  resulting in an increase of 0.4  $\mu\text{mol NH}_4^+ \text{L}^{-1} \text{h}^{-1}$ .~~

216  $\text{C}_{\text{org}}:\text{N}$  ratios of SPM increased during ebb tide (Fig. 4i~~h~~). ~~We observed a~~ A minimum  $\text{C}_{\text{org}}:\text{N}$  ratio of 5.6 around high tide that increased to a maximum of 13.0 during ebb tide was observed. Simultaneously, the SPM concentration increased during ebb tide, from 12.8  $\text{mg L}^{-1}$  SPM to a maximum of 82.4  $\text{mg L}^{-1}$  SPM at the second last station (Table B1).

219

Formatiert: Nicht Hochgestellt/ Tiefgestellt



221

222 **Figure 4** Tidal cycle from high tide to low tide. Temporal distribution of a) total alkalinity (TA), b) dissolved inorganic223 carbon (DIC), c) nitrate, silicate, d) silicate, salinity, e) ammonium, f) calcite saturation state ( $\Omega$ ), g) pH, g) nitrate, h)224 ammonium, i)  $\text{C}_{\text{org}}:\text{N}$  ratio of SPM, and i) DIC:TA ratio from high tide to low tide. Note the different y-axes.

225

### 226 3.3 TA generation

227 The Dutch Wadden Sea is exposed to strong tidal forcing by the North Sea leading to a bi-diurnal exchange of water. The  
228 strong tidal forcing ~~induces a strong~~highlights the benthic-pelagic coupling. ~~Many studies support~~and let us assume that the  
229 outflowing water exports material from the sediment (e.g., Billerbeck et al., 2006; Røy et al., 2008). ~~In order to~~To support our  
230 assumption ~~of a sediment source of TA~~, we further investigated potential TA sources.

231 For a first rough estimate of a maximum TA export during ebb tide, we used the observed TA increase ( $\Delta TA$ ) of  $51.6 \mu\text{mol}$   
232  $\text{kg}^{-1}$  TA during ebb tide (in the Ameland Inlet), and the tidal prism of  $478 \cdot 10^6 \text{ m}^3$  of the Ameland Inlet (Louters and Gerritsen,  
233 1994). With this estimate, we ~~obtained~~ arrived at a rough TA export on the order of  $23.9 \text{ mol TA}$  during ebb tide from the  
234 Ameland Inlet into the North Sea. With an ~~observed~~ tidal duration of 6.8 h, the estimated TA export of  $23.9 \text{ mol}$  would result  
235 in a TA export of  $3.5 \text{ mol h}^{-1}$  TA.

236 ~~For a further source location of the generated TA, we checked various correlations and relations.~~

237 Based on the correlation of TA and silicate ( $R^2 = 0.93$ ), and on the ~~nonlinear~~ relation between both, TA and salinity ( $R^2 =$   
238  $0.32$ ), as well as silicate and salinity ( $R^2 = 0.21$ ), we were able to determine whether TA originates in ~~this part of the~~ Wadden  
239 Sea or is carried by river runoff. Both, TA and silicate increased almost proportionally during ebb tide, pointing to the same  
240 origin (Fig. 5b). The ~~non-conservative behavior similar pattern~~ of TA over salinity and silicate over salinity ~~suggested non-~~  
241 ~~conservative behavior of both, and~~ rules out any sources due to fresh-water dilution and river runoff (Table B1).

242 ~~In order to~~ further ~~elucidated~~shed light on potential TA sources in the Dutch Wadden Sea, we correlated TA with ~~DIC, silicate,~~  
243 ~~nitrate, and ammonium~~ various parameters from high tide to low tide (Fig. 5). The first four samples on the left side of the  
244 plots in Fig. 5 show values probably at the tipping point of high tide, whereby we recommend neglecting these samples in the  
245 interpretation of ebb tide samples. ~~The observation of samples collected during ebb tide allowed us to examine potential sources~~  
246 ~~of TA generation.~~

247 First, ~~we tested~~ the correlation between TA and DIC ~~that~~ reveals the ratio between anaerobic and aerobic processes, ~~which~~  
248 ~~We identified~~ a strong positive correlation between DIC and TA ( $R^2 = 0.93$ ) with TA contents higher than DIC contents (Fig.  
249 5a). However, even with contents of TA higher than DIC, the slope of 1.877 indicated DIC release excess with an increase in  
250 DIC ( $\Delta \text{DIC} = 101.3 \mu\text{mol kg}^{-1}$ ) almost twice as high as TA ( $\Delta \text{TA} = 51.6 \mu\text{mol kg}^{-1}$ ) (Fig. 5a). This may be caused by strong  
251  $\text{CO}_2$  production due to high aerobic OM degradation, or uptake from the atmosphere ~~by enhanced due to~~ water movement ~~by~~  
252 ~~tidal forcing~~. The TA increase can be fueled by various processes which we will discuss ~~below at later stage~~. We detected an  
253 almost linear positive correlation of increasing TA and silicate ( $R^2 = 0.93$ ) during ebb tide, supporting the ~~pore-water~~  
254 ~~outflow out washing process from the pore-water~~ (Fig. 5b). ~~We identified a~~ stronger influence of the pore-water with ongoing  
255 ebb tide ~~is indicated by increasing values~~. The positive correlation between nitrate and TA ( $R^2 = 0.67$ ) (Fig. 5c) was ~~less~~  
256 ~~stronger~~ than the correlations between TA and DIC and TA and Si, which could be traced back on an effect of the first four

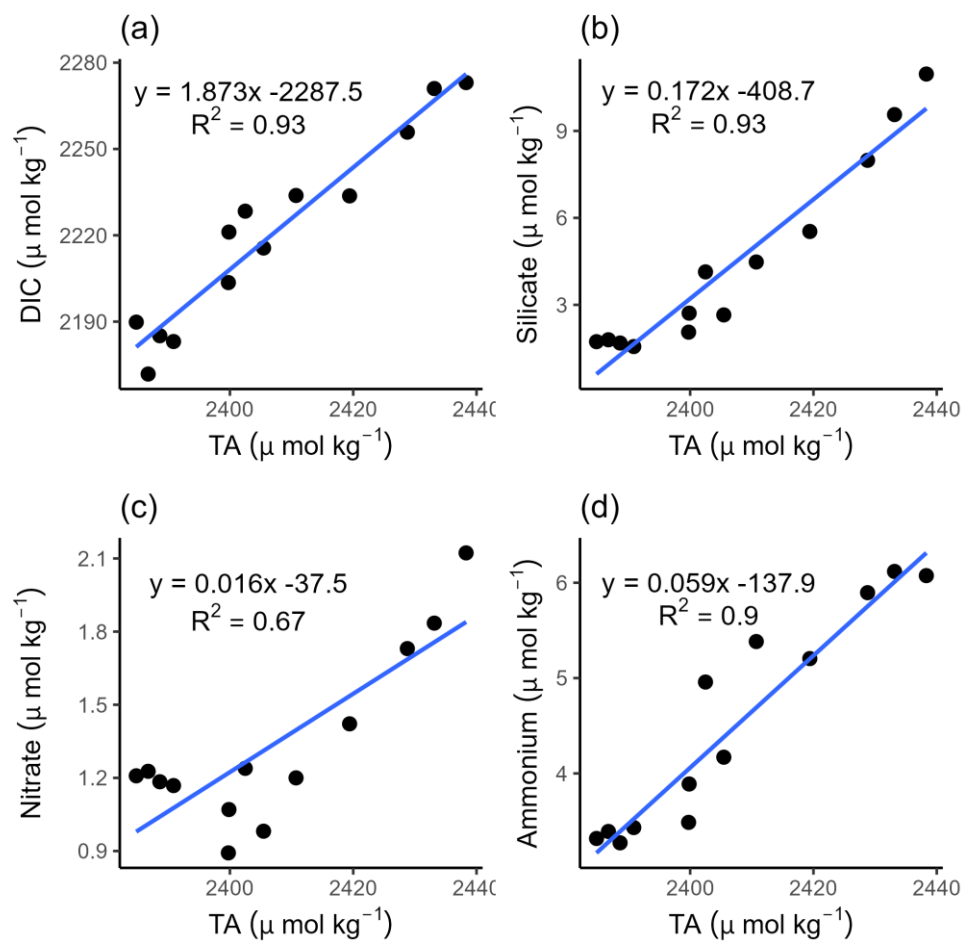
Formatiert: Hochgestellt

Formatiert: Hochgestellt

Formatiert: Hochgestellt

Formatiert: Hochgestellt

257 samplings as mentioned above. In the remaining samples, we observed the increasing nitrate and TA contents, suggesting a  
258 stronger effect of TA generation than nitrate production.



259  
260 **Figure 5** Correlations of TA with a) dissolved inorganic carbon (DIC), b) silicate, c) nitrate, and d) ammonium during ebb  
261 tide in the Ameland Inlet.

## 262 4 Discussion

### 263 4.1 Spatial TA variability

264 ~~In the past,~~ Hoppema (1990) reported TA distributions in the ~~western-most part of the Dutch~~ western Wadden Sea around the  
265 barrier islands Texel, Vlieland, and Terschelling. He focused on the tidal basins drained by the tidal inlets Marsdiep and Vlie  
266 located more ~~to the western~~ than our sampling stations (~~not visible on the map~~). Hoppema (1990) did not observe an increase  
267 of salinity in the Wadden Sea from the fresh-water source towards the ocean and associated this to the influence of tidal  
268 differences ~~and an arbitrary sampling scheme. In most parts of the Wadden Sea we also did not observe salinities. The presence~~  
269 ~~of seawater in the Dutch Wadden Sea and on the tidal flats is supported by our transect data, which show relatively high~~  
270 ~~salinities at coastal North Sea level. Brackish salinities were~~ was only detected in the large Ems Estuary, ~~which receives with~~  
271 high discharges of fresh-water ~~from the river Ems~~, and close to Harlingen and Lauwersoog, which have directly fresh-water  
272 inflows by smaller rivers ~~and streams. Beside this, the Wadden Sea is clearly dominated by coastal North Sea water with~~  
273 ~~relatively high salinities. The presence of seawater in the Wadden Sea and on the tidal flats is supported by our transect data,~~  
274 ~~which show relatively high salinities in the Wadden Sea at the level of the coastal North Sea. The absence of clear salinity~~  
275 ~~gradients in this part of the Dutch Wadden Sea suggest that most of the IJsselmeer discharge was exchanged with the North~~  
276 ~~Sea through the Marsdiep.~~

277 ~~While~~ The spatial TA data by Hoppema (1990), showed lower TA contents at stations with more fresh-water influence and  
278 higher TA contents in the tidal inlets. ~~The data of this study also show we observed~~ high TA contents in the tidal inlets,  
279 ~~suggesting TA generation in sediments, which is fueled by high imports of nutrients and OM (Van Beusekom and De Jonge,~~  
280 ~~2002).~~ The even higher TA contents at stations with lower salinities close to the mainland observed in this study also show  
281 ~~the influence from the catchment area on the coast and TA generation in the shallow sediments near the coast. This result~~  
282 ~~suggests TA generation in sediments, which is fueled by high imports of nutrients and OM.~~ In May (1986), Hoppema's (1990)  
283 data showed TA contents ranging between 2319 and 2444  $\mu\text{mol kg}^{-1}$  TA at salinities between 18.62 and 29.17, while our  
284 lowest observed TA content was 2332  $\mu\text{mol kg}^{-1}$  TA at a salinity of 32.14, and our highest TA content was 2517  $\mu\text{mol kg}^{-1}$   
285 TA at a salinity of 20.25 close to the coastal mainland. Comparing both studies, one can say that the general level of TA was  
286 in a similar range. In addition to the spatial differences, the general level of TA was only slightly higher in our data than in the  
287 data from the early 1990s.

288 A conservative mixing between TA and salinity is only visible in the Ems-Dollard Inlet and the Vlie Inlet (Fig. 3). ~~The~~  
289 ~~conservative mixing For the in the~~ Vlie Inlet, this can be explained by the fact that more ~~North Sea~~ water masses from the  
290 ~~North Sea~~ pass through the deeper inlets and transport more seawater towards the coast. The Vlie Inlet ~~has the is the one with~~  
291 ~~the~~ highest average tidal prism and ~~is~~ the second largest inlet after the Marsdiep Inlet in the Dutch Wadden Sea (Elias et al.,  
292 2012). Similar to our findings, Hoppema (1990) noted a linear mixing of TA and salinity in the Vlie Inlet ~~during his time~~, and  
293 suspected a lower fresh-water ~~contribution~~ there as well.

294 ~~In the~~ Ems-Dollard Inlet, ~~conservative mixing was observed indicating minor contributions from other sources, the~~  
295 ~~Ems River discharges more fresh water and therefore dominates the mixing.~~ In a previous study, Norbistrath et al. (2023)  
296 observed very high TA contents and TA generation in the upper tidal river of the highly turbid Ems Estuary, which may explain  
297 the high levels of TA in the estuary (at low salinities) ~~that we~~ observed in this study.

298 ~~Compared to the past, our initial TA values in the Vlie Inlet sampled in May were somewhat higher than in Hoppema (1990),~~  
299 ~~where he sampled in June and August. His TA values measured in the Marsdiep Inlet in May were in a similar range to ours,~~  
300 ~~but the inlet is located more western with a higher impact from the North Sea and the IJsselmeer.~~

301 Hoppema (1990) also identified varying TA contents within the Dutch Wadden Sea and related these to different sinks and  
302 sources. TA sinks can be calcium carbonate (CaCO<sub>3</sub>) precipitation, or extraction of seawater carbonate by mollusks (e.g., Chen  
303 and Wang, 1999; Hoppema, 1990). Variable fresh-water inflows can either serve as a sink or a source (e.g., Chen and Wang,  
304 1999; Hoppema, 1990). Other sources can be CaCO<sub>3</sub> dissolution, anaerobic metabolic processes in the sediment, or erosion of  
305 TA enhancing sediments (e.g., Hoppema, 1990; Chen and Wang, 1999).

306 Since we ~~almost~~ observed constant marine salinities (> 30), and higher TA values in the Dutch Wadden Sea than in the  
307 North Sea, ~~which is in contrast to~~, we exclude TA sinks and only focus only on TA sources here. According to Hoppema  
308 (1990), the main causes for TA variations in the Dutch Wadden Sea were fresh-water inflows and sources in the sediment. In  
309 our study, fresh-water inflows with high TA contents were only observed in the Ems Estuary and Ems-Dollard Inlet, but not  
310 around the islands and the tidal flats. For a further TA source identification in the Dutch Wadden Sea, we investigated~~observed~~  
311 the TA variability during~~with~~ a tidal cycle close to Ameland.

#### 312 4.2 Determination of TA generation

313 ~~Since identified variations in the Dutch Wadden Sea's TA occurrence and distribution, and~~ Burt et al. (2016) and  
314 ~~Schwichtenberg et al. (2020) assumed TA generation in the Wadden Sea as an important source for the North Sea's carbon~~  
315 storage capacity, Here, we want to further identify ~~shed light on the~~ TA generation and potential TA sources.

316 In a study from the early 1990s, Hoppema (1993) observed a tidal cycle in the Marsdiep in May and September, ~~while he~~  
317 ~~focused~~ on TA, DIC, and oxygen, he. ~~In his study Hoppema (1993), salinity values between 21 and 26, which were lower~~  
318 ~~than ours (> 32), were observed. Hoppema (1993) also observed increasing TA values during ebb tide and assumed the tidal~~  
319 flats and discharging rivers and canals as TA sources, ~~of TA~~.

320 Our present TA data and the historical TA data show no ~~We detected no~~ large differences ~~between our data and the TA values~~  
321 ~~during a tidal cycle observed by~~ in the range of values observed during a tidal cycle. However, an in-depth interpretation and  
322 comparison of both data sets would exceed the capacity of these data, leading us to focus on TA generation during our cruise.

323 ~~Since we observed a generation of 7.6 μmol TA kg<sup>-1</sup> h<sup>-1</sup> during ebb tide, we also support the assumption of the Wadden Sea~~  
324 ~~being a TA source for the North Sea.~~

325 Our observation of a TA generation of 7.6 μmol kg<sup>-1</sup> h<sup>-1</sup> TA during ebb tide supports the assumption of the Wadden Sea being  
326 a TA source for the North Sea. With the tidal prism of the Ameland Inlet estimated by Louters and Gerritsen (1994), we

Feldfunktion geändert

Feldfunktion geändert

327 estimated an ~~upper bound first rough potential maximum~~ TA export from the Dutch Wadden Sea into the North Sea on the  
328 order of 23.9 mol TA during ebb tide ( $3.5 \text{ mol h}^{-1}$  TA) ~~at least~~ between spring and summer. This TA export amount is just a  
329 rough maximum estimate, because some waters in the main tide ~~ways and~~ channels have no direct contact to the areas of the  
330 tidal flats. Schwichtenberg et al. (2020) assumed an annual export of 10 to 14 Gmol yr<sup>-1</sup> TA for the entire Dutch Wadden Sea.  
331 An inclusion of our TA export ~~Since we only have one value of one tidal observation, an inclusion~~ into the model used by  
332 Schwichtenberg et al. (2020) would be unreliable, ~~since it based on only one value of one tidal observation~~ (personal  
333 communication J. Pätsch, 2022). To test whether ~~their observed~~ TA generation match their suggested TA export, more  
334 observational data are required. Therefore, we suggest ~~as future work to collect samples at least in each season seasonal~~  
335 ~~observational data~~ in order to run the model and gain a representative result (personal communication J. Pätsch, 2022) ~~as future~~  
336 ~~work~~.

### 337 4.3 TA source attribution

#### 338 4.3.1 Local sediment outwash

339 In order to gain further ~~insight inside~~ into potential sources of TA, we included nutrients in our investigation. The main focus  
340 was on silicate that we used as a natural tracer since it is not directly provided anthropogenically and allowed us to determine  
341 the silicate source (Van Der Zee and Chou, 2005). ~~In the silicate concentrations, w~~We identified a silicate increase of  $1.4 \mu\text{mol}$   
342  $\text{L}^{-1} \text{h}^{-1}$  Si during ebb tide. Silicate originates from dissolution of diatoms and ~~pore-water exchange sediment outwash~~ in the  
343 Wadden Sea (Van Bennekom et al., 1974; Van Der Zee and Chou, 2005). Here, we relate the silicate increase to outwash from  
344 sediments, because it markedly increased during ebb tide. This assumption ~~is can be~~ supported by Van Bennekom et al. (1974),  
345 who suggested silicate diffusion from interstitial water in the sediment as potential source, since very high silicate  
346 concentrations were found in deeper sediment layers (Rutgers van der Loeff, 1974). Due to the absence of large estuaries  
347 nearby and ~~a~~ salinity consistently ~~being~~ above 32, we exclude fresh-water runoff as a major silicate source. This can be  
348 supported by the relation between silicate and salinity in which we observed a non-conservative behavior (Table B1). Since  
349 TA behaves also non-conservative relative to salinity (Table B1), the ~~silicate observations support the~~ occurrence of TA  
350 sources in the tidal flats of the Wadden Sea. ~~other than river runoff is supported~~.

351 Submarine groundwater discharge (SGD) was identified as a source for nutrient fluxes in tidal flat ecosystems in previous  
352 studies (e.g., Billerbeck et al., 2006; Røy et al., 2008; Santos et al., 2021; Waska and Kim, 2011; Wu et al., 2013). Waska and  
353 Kim (2011) identified strong SGD contributing up to 50 to 70 % of the nutrient fluxes that fuel primary production in a tidal  
354 embayment (Hampyeong Bay) in southwest Korea. In May, they observed low salinities indicating fresh-water. However, in  
355 September they observed constant marine salinities referring them to be exclusively composed of recirculating seawater. Since  
356 we constantly observed marine salinities, we suspect that recirculating marine groundwater enriched with nutrients ~~could~~ act  
357 as a source for our observed increasing TA and nutrients parameters.

Formatiert: Nicht Hochgestellt/ Tiefgestellt



358 TA generation in tidal flats was also observed by Faber et al. (2014), who focused on a large macro tidal embayment in southern  
359 Australia. They also found increasing TA values during ebb tide. ~~Because they used  $^{222}\text{Rn}$  (radon 222) as a conservative~~  
360 ~~tracer to detect pore-water exchange, they were able to~~ associated the TA increase with a higher fraction of pore-water, ~~which~~  
361 ~~contained higher TA contents,~~ and determined the tidal cycle as the controlling force for pore-water exchange. Their findings  
362 ~~This explanation~~ and the observed silicate outwash support our assumption that TA is generated in the sediments of the tidal  
363 flats and is washed out during ebb tide. In addition, we exclude lateral advected signals from more western regions as the Vlie  
364 Inlet, since the TA contents in the surface transect samples in the Vlie Inlet (except of the two samples close to the coastal  
365 mainland near Harlingen) were in the same range as the other observed TA contents and were below the increasing TA contents  
366 during ebb tide. Both increases in TA and silicate are clearly tidal signals, and we clearly identify TA generation in the  
367 sediments of the tidal flats here as local TA sources.

#### 368 4.3.2 TA generating processes

369 The observed TA generation of  $7.6 \mu\text{mol kg}^{-1} \text{h}^{-1}$  TA and the silicate increase of  $1.4 \mu\text{mol L}^{-1} \text{h}^{-1}$  Si indicated an excess of TA  
370 ~~under consideration of given~~ a TA:silicate ratio of 2:1 (Marx et al. 2017), and under the condition of silicate being bound in  
371 minerals, which would then account for a TA generation of  $2.8 \mu\text{mol kg}^{-1} \text{h}^{-1}$  TA. However, when silicate occurred dissolved  
372 in water it does not contribute to TA generation (Meister et al., 2022). A TA excess related to silicate was also observed in the  
373 correlation between TA and silicate (Fig. 5b). Since we observed more TA generated than silicate being washed out, other  
374 biogeochemical processes must be responsible for the TA generation in the sediments of the tidal flats in the Dutch Wadden  
375 Sea.

376  
377 With the observed omega values, we exclude  $\text{CaCO}_3$  dissolution as TA source in the overlying water, since the omega values  
378 were clearly supersaturated with  $\Omega > 1$  (Fig. 4fe, Table B1). The continuous calcite supersaturation nicely indicated the inflow  
379 and dominance of North Sea water during the flood, with omega values similar to previously observed North Sea values ( $\Omega \sim$   
380 3.5 to 4) (Charalampopoulou et al., 2011; Carter et al., 2014). However, because of the  $\Omega$  supersaturation of the overlying water  
381 and a lack of pore-water data, we were unable to determine if TA generation by  $\text{CaCO}_3$  dissolution occurs in deeper sediment  
382 layers. There,  $\text{CaCO}_3$  dissolution can only be driven metabolically, when  $\text{CO}_2$  is produced during OM remineralization or  
383 reduced compounds that were previously produced during anaerobic processes are oxidized and lead to undersaturation with  
384 respect to carbonates (Brenner et al., 2016; Jahnke et al., 1994).

385 ~~By a~~ more detailed interpretation of  $\Delta\text{DIC}$ ,  $\Delta\text{TA}$ , and various nutrient ratios, ~~we tried to~~ further narrow down the potential  
386 sources of TA generation in the sediments and used an upper bound estimate for  $\text{CaCO}_3$  dissolution. The correlation of DIC  
387 and TA reveals an excess of released DIC compared to TA (Fig. 5a), as indicated by the slope of 1.87, while we observed an  
388 increase in DIC ( $\Delta\text{DIC}$ ) almost twice as high as in TA ( $\Delta\text{TA}$ ). The high  $\Delta\text{DIC}$  points to high aerobic OM degradation and  
389 remineralization, resulting in high  $\text{CO}_2$  export. High aerobic OM degradation was also previously observed in the heterotrophic  
390 Wadden Sea (e.g., De Beer et al., 2005; Van Beusekom et al., 1999), assuming an OM degradation and remineralization

391 occurring in the water and sediment in about equal parts (Van Beusekom et al., 1999). High OM degradation is also indicated  
392 by the increasing  $C_{org}:N$  ratios of SPM during ebb tide (Fig. 4h, Table B1). Because we observed constant coastal North Sea  
393 salinities, we rule out fresh-water runoff and terrestrial signals as source for the increasing  $C_{org}:N$  ratios of SPM. We assume  
394 that fresh OM is rapidly degraded, and the older OM settles on and in the sediment where the degradation is continuous and  
395 where it is resuspended by the water exchange with outflowing water. Therefore, we assume that the increase of SPM  
396 concentrations and their  $C_{org}:N$  ratios is an indicator for older and more refractory OM. The increase in TA contents point to  
397 anaerobic processes,  $CaCO_3$  dissolution, or a combination thereof as TA sources occurring in the sediments.

398  
399 For the upper bound estimate, we assumed  $CaCO_3$  dissolution in the sediments with the DIC:TA ratio of 1:2 as source of TA.  
400 Considering this ratio and the observed  $\Delta TA$  of  $51.6 \mu mol kg^{-1}$  TA, a potential  $\Delta DIC$  of  $25.8 \mu mol kg^{-1}$  DIC of the observed  
401  $\Delta TA$  would be produced by  $CaCO_3$  dissolution. The remaining potential  $75.5 \mu mol kg^{-1}$  DIC ( $101.3 - 25.8 \mu mol kg^{-1}$  DIC) of  
402 the observed ( $\Delta DIC$ ) could then be produced by OM degradation and remineralization, and would, using the expected Redfield  
403 ratio of C:N (6.6), correspond to an estimated potential dissolved inorganic nitrogen (DIN) production of  $11.4 \mu mol kg^{-1}$  DIN.  
404 However, this estimated potential DIN production ( $11.4 \mu mol kg^{-1}$  DIN) of OM degradation and remineralization exceeded  
405 the observed increase of  $\Delta DIN$  ( $3.97 \mu mol L^{-1}$  DIN; Table B1, sum of  $NO_3^-$ ,  $NO_2^-$  and  $NH_4^+$ ) during ebb tide. With this  
406 estimation and the assumption that all DIN produced is released and thus lost, TA is probably produced by  $CaCO_3$  dissolution  
407 and anaerobic metabolic processes other than denitrification in the sediment. In addition to that, and with a N-focused  
408 perspective, the DIN loss also hints to the occurrence of other processes that consume nitrogen species but have no net effect  
409 on TA, such as anammox and coupled nitrification-denitrification (Hu and Cai, 2011; Middelburg et al., 2020). The suggested  
410 DIN loss can be supported by considering the marine DIN:Si ratio, which is supposed to be 1:1 (Brzezinski, 1985). We  
411 observed DIN:Si ratios decreasing from 2.7 to 0.8 from high tide to low tide. The decreasing ratios show that both parameter  
412 concentrations increased during ebb tide, whereby DIN concentrations increased lower than silicate concentrations. We  
413 observed a silicate excess with respect to DIN at the end of ebb tide, supporting the DIN loss.

414 Denitrification, the anaerobic irreversible reduction of  $NO_3^-$  to  $N_2$  that generates 0.9 mole TA by using 1 mole  $NO_3^-$  as electron  
415 acceptor (Chen and Wang, 1999) is a net TA source. Denitrification depends on the supply of nitrate, which seasonally varies  
416 (Van Der Zee and Chou, 2005 and references therein). Generally, nitrate is depleted in summer due to high turnover rates and  
417 occurs in higher concentrations in winter (Kieskamp et al., 1991; Jensen et al., 1996; Van Der Zee and Chou, 2005). This  
418 seasonality leads to denitrification rates also being lower in summer and higher in winter (Kieskamp et al., 1991; Jensen et al.,  
419 1996). In previous studies, Faber et al. (2014) identified denitrification as a minor source for TA due to low denitrification  
420 rates, and also Kieskamp et al. (1991) observed low denitrification rates in the Wadden Sea, with low nitrate concentrations  
421 ( $< 2.5 \mu mol L^{-1}$ ) in the overlying water. We observed nitrate concentrations ( $< 2.17 \mu mol L^{-1}$ ) lower than the concentration  
422 sufficient for denitrification assumed by Kieskamp et al. (1991). Therefore, we do not exclude denitrification, but suspect it as  
423 a minor source of TA in the Dutch Wadden Sea at least in spring and summer due to the seasonal lack of nitrate. Thomas et  
424 al. (2009) detected TA seasonality in the southern bight of the North Sea, which is also influenced by the TA generation in the

425 Wadden Sea. We support their findings of lowered TA generation by denitrification in late spring and early summer. In  
426 addition, the calculated potential DIN excess compared to the observed DIN not only hints to other N consuming processes  
427 that have no effect on TA, but also suggests that allochthonous nitrate would be needed to fuel the TA increase by  
428 denitrification. In addition, the albeit low availability of nitrate indicates to predominantly aerobic metabolic activity during  
429 the time of our observations, which is in line with earlier studies reporting an enhanced relevance of anaerobic activity later in  
430 summer (Luff and Moll, 2004; Thomas et al., 2009).

431  
432 Another source of TA in sediments is aerobic OM respiration with the associated formation of ammonium while consuming  
433  $H^+$  (Blackburn and Henriksen, 1983; Berner et al., 1970; Brenner et al., 2016). The observed increasing ammonium  
434 concentrations (Fig. 4e) could be associated with aerobic OM degradation leading to ammonium formation. The resulting  
435 ammonium formation in the upper oxygenated sediment layers would increase DIC by the production of  $CO_2$ , and increase  
436 TA by the consumption of  $H^+$  (Fig. 5) (Brenner et al., 2016). In sediments, the production of one mole ammonium (from  
437 ammonia) would then generate one mole TA (Berner et al., 1970; Meister et al., 2022). In contrast, in the water column, the  
438 aerobic respiration of OM produce  $CO_2$  and increase DIC, also visible in decreasing pH values (Fig. 4g), but consume TA  
439 and would not produce ammonium (Chen and Wang, 1999). Therefore, aerobic OM respiration in the water column could only  
440 explain the higher increase in DIC than in TA, but not the simultaneous increase in TA and ammonium (Fig. 5). Based on this,  
441 we assume that OM respiration associated with TA generation occurs in the sediments, leading to TA and DIC generation and  
442 also to ammonium production, being washed-out during ebb tide. The produced ammonium is then also accessible for  
443 nitrification that produces nitrate. A slightly increased nitrate concentration in the most upper sediment layers was observed  
444 by Beck et al. (2008a) in the German Wadden Sea. This observation, a potential nitrate reservoir, nitrate production due to OM  
445 degradation and nitrification occurring in the upper oxygenated sediment layers (Martin and Sayles, 1996), or a  
446 ~~combination~~ thereof could explain the observed low increasing nitrate concentrations during ebb tide. However, as we rule  
447 out terrestrial nitrate imports as nitrate source here, the simultaneous increase of TA and nitrate is noticeable for us, because  
448 nitrification consumes TA (Brenner et al., 2016). We assume that potential nitrification has a minor effect on TA, since we  
449 observed only low nitrate concentrations and a really low increase of nitrate compared to the increase of ammonium and TA  
450 during ebb tide. ~~The~~ Low nitrate concentrations resulting in a reduced availability of bound oxygen, i.e., electron acceptors.  
451 This promotes the occurrence of other anaerobic processes of the redox system to generate TA in the deeper, anoxic sediment  
452 layers in the Dutch Wadden Sea, such as sulfate and iron reduction.

453 Sulfate reduction followed by iron reduction and the formation and burial of pyrite are net sources of TA, since TA  
454 consumption by reoxidation is excluded when buried in sediments (Berner et al., 1970; Faber et al., 2014). Whether these  
455 processes contribute to TA generation in the deeper sediments of the Dutch Wadden Sea cannot be further identified without  
456 the necessary data. However, sulfate reduction was also mentioned as source of TA by Thomas et al. (2009). The temporary  
457 slight appearance of noticeable sulfuric odor could be another indirect indicator for the occurrence of sulfate reduction. In  
458 previous studies of tidal flats in the German Wadden Sea, Beck et al. (2008a); (2008b) observed increasing TA contents with

459 depth and identified sulfate reduction as the most important process for anaerobic OM remineralization in pore-water cores.  
460 Sulfate reduction releases 1.14 mole TA with the oxidation of one mole carbon of POC, and iron reduction releases 8.14 mole  
461 TA with the oxidation of one mole carbon of POC, indicating that both processes are large sources of TA generation (Brenner  
462 et al., 2016), but ~~cannot be further~~ studies are needed to support this, interpreted without the necessary data.  
463

464 A strict comparison of the northern and the western parts of the Wadden Sea ~~is difficult~~cannot be fully recommended because  
465 the areas vary in terms of OM import and eutrophication effects (Van Beusekom et al., 2019), sediment composition, and  
466 extent between the barrier islands and the mainland, all of which influence the occurrence and interaction of biogeochemical  
467 processes (Schwichtenberg et al., 2020). ~~Although,~~ The area characteristics of the northern and western Wadden Sea differ  
468 especially in terms of OM turnover being lower in the norther Wadden Sea. ~~As~~ previous study by Brasse et al. (1999)  
469 identified high TA and DIC contents in the sediment of the North Frisian Wadden Sea and identified CaCO<sub>3</sub> dissolution and  
470 sulfate reduction as major TA sources, which ~~is appear~~ consistent with our findings.

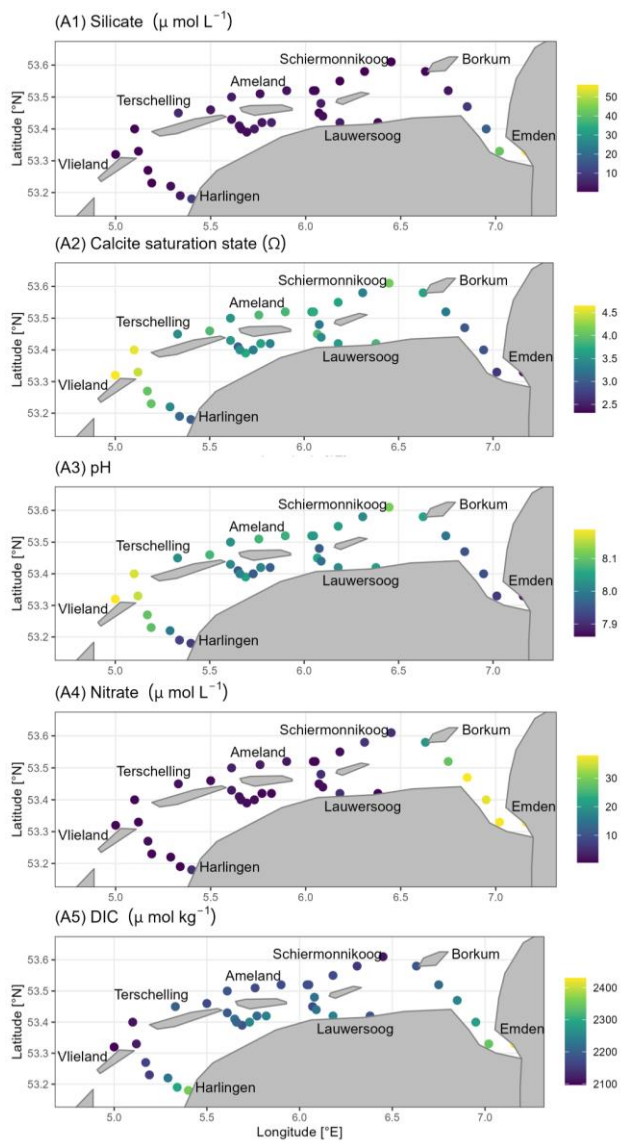
## 471 5 Conclusion

472 The Dutch Wadden Sea is a unique and highly dynamic ecosystem. While observing the spatial TA distribution and TA  
473 generation in the Dutch Wadden Sea, we detected higher TA values than in the North Sea, and identified the Dutch Wadden  
474 Sea clearly as a TA source ~~for~~ the North Sea's carbonate system. Compared to ~~previous historical~~ studies (Hoppema, 1990,  
475 1993), the TA values we observed were in a similar range, with high TA values in the tidal basins. Beside the need for seasonal  
476 observations, future work should also focus on the tidal end-members to better understand the general and seasonal influence  
477 of freshwater inflows on the TA status in the Dutch Wadden Sea. ~~but while he observed lower TA values near the coast, we~~  
478 ~~found higher ones there. However, more data from various seasons would be needed for a better comparison between then and~~  
479 ~~now, and for a more precise status of TA.~~

480 By observing salinity and using silicate as a tracer, we excluded fresh-water dilution and river runoff as TA sources on the  
481 tidal flats, and instead, identified local outwash from the tidal flat sediments as sources of TA. Aerobic, metabolic processes  
482 such as CaCO<sub>3</sub> dissolution and ammonium formation seem to dominate TA generation in the upper oxic sediment layers and  
483 the overlying water, while anaerobic, metabolic processes such as denitrification, sulfate and iron reduction are potential TA  
484 sources in the deeper anoxic sediment layers. However, in spring and early summer, denitrification seems to play a minor role  
485 in generating TA in the sediments of the Dutch Wadden Sea due to seasonality and associated limited nitrate availability.

486 **6 Appendices**

487 **Appendix A**



489 **Figure A** Latitudinal and longitudinal distribution of A1) silicate (Si;  $\mu\text{mol L}^{-1}$ ), A2) calcite saturation state ( $\Omega$ ), A3) pH, A4)  
 490 nitrate ( $\text{NO}_3^-$ ;  $\mu\text{mol L}^{-1}$ ), and A5) dissolved inorganic carbon (DIC;  $\mu\text{mol kg}^{-1}$ ) from surface water samples in May 2019.

#### 491 **Appendix B**

492 **Table B1** Tidal cycle sample parameter during ebb tide. Sample no. 545 is the first sample at high tide and sample no. 557 is  
 493 the last sample at ebb tide on May 21<sup>st</sup> 2019. Shown are rounded up values of temperature (Temp), salinity (Sal), total alkalinity  
 494 (TA), dissolved inorganic carbon (DIC), silicate (Si), nitrate ( $\text{NO}_3^-$ ), nitrite ( $\text{NO}_2^-$ ), ammonium ( $\text{NH}_4^+$ ), dissolved inorganic  
 495 nitrogen (DIN), the amount of carbon (C) and organic carbon ( $\text{C}_{\text{org}}$ ) of SPM, the amount of nitrogen (N) of SPM, the calcite  
 496 (Ca) and aragonite (Ar) saturation states, the pH, and phosphate ( $\text{PO}_4^{3-}$ ) per sample.

Sample No.	Temp [°C]	Sal	TA [ $\mu\text{mol kg}^{-1}$ ]	DIC [ $\mu\text{mol kg}^{-1}$ ]	Si [ $\mu\text{mol L}^{-1}$ ]	$\text{NO}_3^-$ [ $\mu\text{mol L}^{-1}$ ]	$\text{NO}_2^-$ [ $\mu\text{mol L}^{-1}$ ]	$\text{NH}_4^+$ [ $\mu\text{mol L}^{-1}$ ]
545	13.26	32.52	2387	2172	1.84	1.26	0.19	3.47
546	13.25	32.52	2385	2190	1.77	1.24	0.19	3.40
547	13.28	32.52	2389	2185	1.72	1.21	0.19	3.35
548	13.38	32.52	2391	2183	1.6	1.19	0.19	3.52
549	14.32	32.50	2400	2204	2.11	0.91	0.25	3.57
550	14.61	32.50	2400	2221	2.78	1.09	0.29	3.98
551	14.64	32.51	2405	2216	2.72	1.01	0.29	4.27
552	14.73	32.51	2411	2234	4.59	1.23	0.34	5.51
553	14.77	32.51	2402	2228	4.24	1.26	0.33	5.08
554	14.72	32.51	2419	2234	5.66	1.46	0.36	5.33
555	14.66	32.51	2428	2256	8.18	1.77	0.43	6.04
556	14.68	32.51	2433	2271	9.79	1.87	0.47	6.27
557	14.70	32.50	2438	2273	11.22	2.17	0.50	6.22
Sample No.	DIN [ $\mu\text{mol L}^{-1}$ ]	C / $\text{C}_{\text{org}}$ (SPM) [ $\mu\text{mol L}^{-1}$ ]	N (SPM) [ $\mu\text{mol L}^{-1}$ ]	$\text{C}_{\text{org}}:\text{N}$ (SPM)	SPM [ $\text{mg L}^{-1}$ ]	Ca / Ar [ $\Omega$ ]	pH	$\text{PO}_4^{3-}$ [ $\mu\text{mol L}^{-1}$ ]
545	4.93	86.8 / 65.1	8.8	7.4	12.8	3.8 / 2.4	8.07	0.12
546	4.83	72.7 / 42.4	7.4	5.8	8.7	3.5 / 2.3	8.03	0.11
547	4.76	112.4 / 93.4	9.6	9.7	15.4	3.7 / 2.3	8.05	0.11
548	4.91	108.5 / 104.6	9.9	10.5	16.8	3.7 / 2.4	8.05	0.12
549	4.73	111.1 / 97.8	8.8	11.1	13.9	3.6 / 2.3	8.01	0.32
550	5.37	233.0 / 180.3	17.7	10.2	32.2	3.3 / 2.1	7.97	0.42
551	5.56	193.2 / 174.3	14.5	12.0	29.6	3.5 / 2.2	7.99	0.47
552	7.08	248.6 / 163.5	18.4	8.9	34.3	3.3 / 2.1	7.96	0.57
553	6.67	257.6 / 199.3	18.3	10.9	41.6	3.2 / 2.1	7.95	0.54
554	7.15	324.4 / 271.1	23.2	11.7	55.0	3.4 / 2.2	7.98	0.54

555	8.24	440.4 / 345.2	29.2	11.8	75.7	3.2 / <u>2.1</u>	7.95	0.58
556	8.61	430.5 / 363.3	27.9	13.0	82.4	3.1 / <u>2.0</u>	7.93	0.62
557	8.90	308.9 / 199.1	21.2	9.4	48.8	3.1 / <u>2.0</u>	7.93	0.63

#### 497 **Data availability**

498 The data of this study are either presented in the article or are available upon request from the corresponding author.

#### 499 **Author Contributions**

500 MN wrote the manuscript, did the carbon sampling and sample measurement, analyzed and evaluated the data, and led the  
501 study. JvB led the research cruise. JvB and HT contributed with editorial and scientific recommendations. MN prepared the  
502 manuscript with contribution from all co-authors.

#### 503 **Competing interests**

504 The contact author has declared that none of the authors has any competing interests.

#### 505 **Acknowledgement**

506 We thank the crew from RV *Ludwig Prandtl* for their support during the cruise. We thank Leon Schmidt for the nutrient  
507 sampling and measurements, and Marc Metzke for the C/N measurements. We further thank Xiping Hu and two anonymous  
508 reviewers for their constructive comments, which greatly improved this manuscript.

#### 509 **Financial support**

510 This research has been funded by the German Academic Exchange Service (DAAD, project: MOPGA-GRI, grant no.  
511 57429828), which received funds from the German Federal Ministry of Education and Research (BMBF).

#### 512 **References**

513 Abril, G., and Frankignoulle, M.: Nitrogen–alkalinity interactions in the highly polluted Scheldt basin (Belgium), Water Research, 35, 844–  
514 850, [https://doi.org/10.1016/S0043-1354\(00\)00310-9](https://doi.org/10.1016/S0043-1354(00)00310-9), 2001.  
515 Beck, M., Dellwig, O., Holstein, J. M., Grunwald, M., Liebezeit, G., Schnetger, B., and Brumsack, H.-J.: Sulphate, dissolved organic carbon,  
516 nutrients and terminal metabolic products in deep pore waters of an intertidal flat, Biogeochemistry, 89, 221–238,  
517 <https://doi.org/10.1007/s10533-008-9215-6>, 2008a.

Formatiert: Englisch (Vereinigte Staaten)

Formatiert: Englisch (Vereinigte Staaten)

Feldfunktion geändert

Formatiert: Englisch (Vereinigte Staaten)

Feldfunktion geändert

Formatiert: Englisch (Vereinigte Staaten)

Formatiert: Englisch (Vereinigte Staaten)





574 Hoppema, J.: The distribution and seasonal variation of alkalinity in the southern bight of the North Sea and in the western Wadden Sea,  
575 Netherlands journal of sea research, 26, 11-23, [https://doi.org/10.1016/0077-7579\(90\)90053-J](https://doi.org/10.1016/0077-7579(90)90053-J), 1990.

576 Hoppema, J.: The oxygen budget of the western Wadden Sea, The Netherlands, Estuarine, Coastal and Shelf Science, 32, 483-502,  
577 [https://doi.org/10.1016/0272-7714\(91\)90036-B](https://doi.org/10.1016/0272-7714(91)90036-B), 1991.

578 Hoppema, J.: Carbon dioxide and oxygen disequilibrium in a tidal basin (Dutch Wadden Sea), Netherlands journal of sea research, 31, 221-  
579 229, [https://doi.org/10.1016/0077-7579\(93\)90023-1](https://doi.org/10.1016/0077-7579(93)90023-1), 1993.

580 Hu, X., and Cai, W. J.: An assessment of ocean margin anaerobic processes on oceanic alkalinity budget, Global Biogeochemical Cycles,  
581 25, doi.org/10.1029/2010GB003859, 2011.

582 Jahnke, R. A., Craven, D. B., and Gaillard, J.-F.: The influence of organic matter diagenesis on CaCO<sub>3</sub> dissolution at the deep-sea floor,  
583 Geochimica et Cosmochimica Acta, 58, 2799-2809, 1994.

584 Jensen, K., Jensen, M., and Kristensen, E.: Nitrification and denitrification in Wadden Sea sediments (Königshafen, Island of Sylt, Germany)  
585 as measured by nitrogen isotope pairing and isotope dilution, Aquatic Microbial Ecology, 11, 181-191, doi:10.3354/ame011181, 1996.

586 Keith, D. W., Ha-Duong, M., and Stolaroff, J. K.: Climate strategy with CO<sub>2</sub> capture from the air, Climatic Change, 74, 17-45,  
587 <https://doi.org/10.1007/s10584-005-9026-x>, 2006.

588 Kérouel, R., and Aminot, A.: Fluorometric determination of ammonia in sea and estuarine waters by direct segmented flow analysis, Marine  
589 Chemistry, 57, 265-275, [https://doi.org/10.1016/S0304-4203\(97\)00040-6](https://doi.org/10.1016/S0304-4203(97)00040-6), 1997.

590 Kieskamp, W. M., Lohse, L., Epping, E., and Helder, W.: Seasonal variation in denitrification rates and nitrous oxide fluxes in intertidal  
591 sediments of the western Wadden Sea, Marine ecology progress series. Oldendorf, 72, 145-151, 1991.

592 Lewis, E., and Wallace, D.: Program developed for CO<sub>2</sub> system calculations, Environmental System Science Data Infrastructure for a Virtual  
593 Ecosystem, 1998.

594 Louters, T., and Gerritsen, F.: The Riddle of the Sands: A Tidal System's Answer to a Rising Sea Level, report RIKZ-94.040 (isbn 90-369-  
595 0084-0), 1994.

596 Luff, R., and Moll, A.: Seasonal dynamics of the North Sea sediments using a three-dimensional coupled sediment-water model system,  
597 Continental Shelf Research, 24, 1099-1127, <https://doi.org/10.1016/j.csr.2004.03.010>, 2004.

598 Martin, W., and Sayles, F.: CaCO<sub>3</sub> dissolution in sediments of the Ceara Rise, western equatorial Atlantic, Geochimica et Cosmochimica  
599 Acta, 60, 243-263, [https://doi.org/10.1016/0016-7037\(95\)00383-5](https://doi.org/10.1016/0016-7037(95)00383-5), 1996.

600 Matthews, H. D., and Caldeira, K.: Stabilizing climate requires near-zero emissions, Geophysical research letters, 35,  
601 <https://doi.org/10.1029/2007GL032388>, 2008.

602 Mehrbach, C., Culbertson, C., Hawley, J., and Pytkowicz, R.: Measurement of the apparent dissociation constants of carbonic acid in seawater  
603 at atmospheric pressure. Limnology and oceanography, 18, 897-907, <https://doi.org/10.4319/lo.1973.18.6.0897>, 1973.

604 Meister, P., Herda, G., Petrishcheva, E., Gier, S., Dickens, G. R., Bauer, C., and Liu, B.: Microbial Alkalinity Production and Silicate  
605 Alteration in Methane Charged Marine Sediments: Implications for Porewater Chemistry and Diagenetic Carbonate Formation, Geochemical  
606 Signals in Dynamic Sedimentary Systems Along Continental Margins, 2022.

607 Meybeck, M.: Global chemical weathering of surficial rocks estimated from river dissolved loads, American journal of science, 287, 401-  
608 428, 10.2475/ajs.287.5.401, 1987.

609 Middelburg, J. J., Soetaert, K., and Hagens, M.: Ocean alkalinity, buffering and biogeochemical processes, Reviews of Geophysics, 58,  
610 e2019RG000681, <https://doi.org/10.1029/2019RG000681>, 2020.

611 Norbistrath, M., Pätsch, J., Dähnke, K., Sanders, T., Schulz, G., van Beusekom, J. E., and Thomas, H.: Metabolic alkalinity release from  
612 large port facilities (Hamburg, Germany) and impact on coastal carbon storage, Biogeosciences, 19, 5151-5165, <https://doi.org/10.5194/bg-19-5151-2022>, 2022.

613 Norbistrath, M., Neumann, A., Dähnke, K., Sanders, T., Schöl, A., van Beusekom, J. E., and Thomas, H.: Alkalinity and nitrate dynamics  
614 reveal dominance of anammox in a hyper-turbid estuary, Biogeosciences, 20, 4307-4321, <https://doi.org/10.5194/bg-20-4307-2023>, 2023.

615 Petersen, W., Schroeder, F., and Bockelmann, F.-D.: FerryBox-Application of continuous water quality observations along transects in the  
616 North Sea, Ocean Dynamics, 61, 1541-1554, <https://doi.org/10.1007/s10236-011-0445-0>, 2011.

617 Postma, H.: Hydrography of the Dutch Wadden sea, Arch. Neerl. Zool, 10, 405-511, 1954.

618 Renforth, P., and Henderson, G.: Assessing ocean alkalinity for carbon sequestration, Reviews of Geophysics, 55, 636-674,  
619 <https://doi.org/10.1002/2016RG000533>, 2017.

620 Ridderinkhof, H., Zimmerman, J., and Philippart, M.: Tidal exchange between the North Sea and Dutch Wadden Sea and mixing time scales  
621 of the tidal basins, Netherlands Journal of Sea Research, 25, 331-350, [https://doi.org/10.1016/0077-7579\(90\)90042-F](https://doi.org/10.1016/0077-7579(90)90042-F), 1990.

622 Røy, H., Lee, J. S., Jansen, S., and de Beer, D.: Tide-driven deep pore-water flow in intertidal sand flats, Limnology and oceanography, 53,  
623 1521-1530, <https://doi.org/10.4319/lo.2008.53.4.1521>, 2008.

624 Rutgers van der Loeff, M.: Transport van reactief silikaat uit Waddenzee sediment naar het bovenstaande water, NIOZ-rapport, 1974.

625 Sabine, C. L., Feely, R. A., Gruber, N., Key, R. M., Lee, K., Bullister, J. L., Wanninkhof, R., Wong, C., Wallace, D. W., and Tilbrook, B.:  
626 The oceanic sink for anthropogenic CO<sub>2</sub>, science, 305, 367-371, DOI: 10.1126/science.1097403, 2004.

Formatiert: Englisch (Vereingite Staaten)

Formatiert

Feldfunktion geändert

Feldfunktion geändert

Formatiert

Feldfunktion geändert

Formatiert

Feldfunktion geändert

Formatiert

Feldfunktion geändert

Formatiert

Feldfunktion geändert

Formatiert

Feldfunktion geändert

Formatiert

Feldfunktion geändert

Formatiert

Feldfunktion geändert

Formatiert

Feldfunktion geändert

Formatiert

Feldfunktion geändert

Formatiert

Feldfunktion geändert

Formatiert: Englisch (Vereingite Staaten)

Formatiert: Englisch (Vereingite Staaten)

Feldfunktion geändert

Formatiert

Feldfunktion geändert

Formatiert

Feldfunktion geändert

Formatiert

Feldfunktion geändert

Formatiert

Feldfunktion geändert

Formatiert

628 Santos, I. R., Chen, X., Lecher, A. L., Sawyer, A. H., Moosdorf, N., Rodellas, V., Tamborski, J., Cho, H.-M., Dimova, N., and Sugimoto,  
629 R.: Submarine groundwater discharge impacts on coastal nutrient biogeochemistry, *Nature Reviews Earth & Environment*, 2, 307-323,  
630 <https://doi.org/10.1038/s43017-021-00152-0>, 2021.

631 Schwichtenberg, F., Callies, U., and van Beusekom, J. E.: Residence times in shallow waters help explain regional differences in Wadden  
632 Sea eutrophication, *Geo-Marine Letters*, 37, 171-177, <https://doi.org/10.1007/s00367-016-0482-2>, 2017.

633 Schwichtenberg, F., Pätsch, J., Böttcher, M. E., Thomas, H., Winde, V., and Emeis, K.-C.: The impact of intertidal areas on the carbonate  
634 system of the southern North Sea, *Biogeosciences*, 17, 4223-4245, <https://doi.org/10.5194/bg-17-4223-2020>, 2020.

635 Shadwick, E., Thomas, H., Gratton, Y., Leong, D., Moore, S., Papakyriakou, T., and Prowe, A.: Export of Pacific carbon through the Arctic  
636 Archipelago to the North Atlantic, *Continental Shelf Research*, 31, 806-816, <https://doi.org/10.1016/j.csr.2011.01.014>, 2011.

637 Suchet, P. A., and Probst, J.-L.: Modelling of atmospheric CO<sub>2</sub> consumption by chemical weathering of rocks: application to the Garonne,  
638 Congo and Amazon basins, *Chemical Geology*, 107, 205-210, DOI:10.1016/0009-2541(93)90174-H, 1993.

639 Thomas, H., Bozec, Y., Elkalay, K., and De Baar, H. J.: Enhanced open ocean storage of CO<sub>2</sub> from shelf sea pumping, *Science*, 304, 1005-  
640 1008, DOI: 10.1126/science.1095491, 2004.

641 Thomas, H., Schiettecatte, L.-S., Suykens, K., Koné, Y., Shadwick, E., Prowe, A. F., Bozec, Y., de Baar, H. J., and Borges, A.: Enhanced  
642 ocean carbon storage from anaerobic alkalinity generation in coastal sediments, *Biogeosciences*, 6, 267-274, <https://doi.org/10.5194/bg-6-267-2009>, 2009.

643 Van Bennekom, A., Krijgsman-van Hartingsveld, E., Van der Veer, G., and Van Voorst, H.: The seasonal cycles of reactive silicate and  
644 suspended diatoms in the Dutch Wadden Sea, *Netherlands Journal of Sea Research*, 8, 174-207, [https://doi.org/10.1016/0077-7579\(74\)90016-7](https://doi.org/10.1016/0077-7579(74)90016-7), 1974.

645 Van Beusekom, J., Brockmann, U., Hesse, K.-J., Hickel, W., Poremba, K., and Tillmann, U.: The importance of sediments in the  
646 transformation and turnover of nutrients and organic matter in the Wadden Sea and German Bight, *Deutsche Hydrografische Zeitschrift*, 51,  
647 245-266, 10.1007/BF02764176, 1999.

648 Van Beusekom, J., and De Jonge, V.: Long-term changes in Wadden Sea nutrient cycles: importance of organic matter import from the  
649 North Sea, in: *Nutrients and Eutrophication in Estuaries and Coastal Waters*, Springer, 185-194, 2002.

650 Van Beusekom, J. E., Buschbaum, C., and Reise, K.: Wadden Sea tidal basins and the mediating role of the North Sea in ecological processes:  
651 scaling up of management?, *Ocean & coastal management*, 68, 69-78, <https://doi.org/10.1016/j.ocecoaman.2012.05.002>, 2012.

652 Van Beusekom, J. E., Carstensen, J., Dolch, T., Grage, A., Hofmeister, R., Lenhart, H., Kerimoglu, O., Kolbe, K., Pätsch, J., and Rick, J.:  
653 Wadden Sea Eutrophication: long-term trends and regional differences, *Frontiers in Marine Science*, 6, 370,  
654 doi.org/10.3389/fmars.2019.00370, 2019.

655 Van Der Zee, C., and Chou, L.: Seasonal cycling of phosphorus in the Southern Bight of the North Sea, *Biogeosciences*, 2, 27-42,  
656 <https://doi.org/10.5194/bg-2-27-2005>, 2005.

657 van Raaphorst, W., and van der Veer, H. W.: The phosphorus budget of the Marsdiep tidal basin (Dutch Wadden Sea) in the period 1950–  
658 1985: importance of the exchange with the North Sea, in: *North Sea—Estuaries Interactions*, Springer, 21-38, 1990.

659 Voynova, Y. G., Petersen, W., Gehrung, M., Aßmann, S., and King, A. L.: Intertidal regions changing coastal alkalinity: The Wadden Sea–  
660 North Sea tidally coupled bioreactor, *Limnology and Oceanography*, 64, 1135-1149, 2019.

661 Wang, Z. A., Kroeger, K. D., Ganju, N. K., Gonnee, M. E., and Chu, S. N.: Intertidal salt marshes as an important source of inorganic  
662 carbon to the coastal ocean, *Limnology and Oceanography*, 61, 1916-1931, 2016.

663 Waska, H., and Kim, G.: Submarine groundwater discharge (SGD) as a main nutrient source for benthic and water-column primary  
664 production in a large intertidal environment of the Yellow Sea, *Journal of Sea Research*, 65, 103-113,  
665 <https://doi.org/10.1016/j.seares.2010.08.001>, 2011.

666 Wolf-Gladrow, D. A., Zeebe, R. E., Klaas, C., Körtzinger, A., and Dickson, A. G.: Total alkalinity: The explicit conservative expression and  
667 its application to biogeochemical processes, *Marine Chemistry*, 106, 287-300, <https://doi.org/10.1016/j.marchem.2007.01.006>, 2007.

668 Wu, Z., Zhou, H., Zhang, S., and Liu, Y.: Using <sup>222</sup>Rn to estimate submarine groundwater discharge (SGD) and the associated nutrient fluxes  
669 into Xiangshan Bay, East China Sea, *Marine pollution bulletin*, 73, 183-191, <https://doi.org/10.1016/j.marpolbul.2013.05.024>, 2013.

670 Zalasiewicz, J., Williams, M., Steffen, W., and Crutzen, P.: *The new world of the Anthropocene*. ACS Publications, 2010.

671 Zhang, C., Shi, T., Liu, J., He, Z., Thomas, H., Dong, H., Rinkevich, B., Wang, Y., Hyun, J.-H., and Weinbauer, M.: Eco-engineering  
672 approaches for ocean negative carbon emission, *Science Bulletin*, 67, 2564-2573, <https://doi.org/10.1016/j.scib.2022.11.016>, 2022.

673

Feldfunktion geändert

Formatiert: Englisch (Vereinigte Staaten)

Formatiert: Englisch (Vereinigte Staaten)

Formatiert: Englisch (Vereinigte Staaten)

Feldfunktion geändert

Formatiert: Englisch (Vereinigte Staaten)

Formatiert: Englisch (Vereinigte Staaten)

Formatiert: Englisch (Vereinigte Staaten)

Feldfunktion geändert

Formatiert: Englisch (Vereinigte Staaten)

Formatiert: Englisch (Vereinigte Staaten)

Feldfunktion geändert

Formatiert: Englisch (Vereinigte Staaten)

Formatiert: Englisch (Vereinigte Staaten)

Feldfunktion geändert

Formatiert: Englisch (Vereinigte Staaten)

Formatiert: Englisch (Vereinigte Staaten)

Feldfunktion geändert

Formatiert: Englisch (Vereinigte Staaten)

Formatiert: Englisch (Vereinigte Staaten)

Feldfunktion geändert

Formatiert: Englisch (Vereinigte Staaten)

Formatiert: Englisch (Vereinigte Staaten)

Feldfunktion geändert

Formatiert: Englisch (Vereinigte Staaten)

Formatiert: Englisch (Vereinigte Staaten)

Feldfunktion geändert

Formatiert: Englisch (Vereinigte Staaten)

Formatiert: Englisch (Vereinigte Staaten)

Feldfunktion geändert

Formatiert: Englisch (Vereinigte Staaten)

Formatiert: Englisch (Vereinigte Staaten)